A Novel Magnetometer Calibration Approach with Artificial Data

Nhan Nguyen
Information Technology and Communication Sciences Faculty
Tampere University
Tampere, Finland
nhan.nguyen@tuni.fi

Philipp Müller
Information Technology and Communication Sciences Faculty
Tampere University
Tampere, Finland
philipp.muller@tuni.fi

Abstract—**This paper proposes two methods for calibrating triaxial magnetometers. Both of them calibrate these sensors with more general assumption of noise on three axes than previous state-of-the-art methods. The first method estimates bias and rotation parameters more accurately and the second method yields a better estimate for the scaling parameter than the state-of-the-art method subMLE. The computational time of the latter is also 43 times faster than subMLE, which allows this method to be applied in devices with low-computational resources (e.g. smartphones). Furthermore, the second method yields more robust heading angle estimates compared to subMLE. This result implies that the second method can be applied in light-weight inertial measurement systems, for which the orientation of the device is vital information for pedestrian dead reckoning system.**

Keywords—magnetometer, calibration, inertial navigation, noise, maximum likelihood estimator

I. INTRODUCTION

Smartphone usage has become indispensable in everyday life. People carry their smartphones with them all the time, which allows determining the position of users based on signals received by their smartphones. Knowing one's position is essential for location-based services (LBS) such as forecasting weather or suggesting nearby shop.

Global Navigation Satellite System (GNSS) provides mobile phones measurements by which they can determine their location with extremely high accuracy in outdoor environments. However, the signals from satellites are reflected by high buildings and get degraded significantly for indoor environments. These limitations have been extensively studied in the literature to find the alternating solutions. Network based methods can also find the position of user by wireless network technologies as in [1]. These methods use, for example, signal strength or angle of arrival from the device to anchor points and then use fingerprinting or trilateration to estimate the location of the device. The limitations are the burden of designing the network and multi-path effects of signals. An alternative solution are sensor-based methods where only sensors integrated in the device are used to estimate the user's location. Indeed, Inertial Measurement Units (IMUs) that consist of multiple sensors such as accelerometer, gyroscope and magnetometer are commonly integrated in nowadays smartphones. These sensors are used to estimate the distance of moving and heading direction of user from the initial location [2].

The magnetometer is used to measure magnetic fields nearby. In outdoor environments, the geomagnetic field is usually observed. Measurements of the geomagnetic field

from the magnetometer can be used to estimate the local North direction and determine the heading direction of the device. However, measurements from the magnetometer are corrupted by multiple error sources and electrical noise. Using the raw measurements directly leads to wrong estimation of heading direction. A calibration procedure is, thus, essential.

Multiple methods to calibrate magnetometers have been studied. The simplest one is swing method [3] that requires the known orientation of the device and is inapplicable in general. Another method that is free from knowledge of the attitude of the devices are in [4]-[6]. The initial derivation was in Least Square scheme [4]. Later derivation also included the model of noise in magnetometer to robustly estimate calibration parameters of the magnetometer under Maximum Likelihood Estimator (MLE) framework, which is heavy computationally demanding. When combining with inertial sensors, [7] can calibrate the magnetometer by lower computational method.

In smartphones, computational resources and provided energy by a battery are limited. Therefore, a method with low computational cost that also uses no information from other sensors is needed. An effective state-of-the-art method is presented in [5]. In our paper, the method from [5] is called as subMLE because the magnetometer is calibrated by a suboptimal MLE method under the assumption that noise in all three axes follows the Gaussian distribution with same parameters. We compare subMLE to our proposed methods.

This paper is an extension of [8] that introduced our work on modeling noise in magnetometers integrated in smartphones. In [8], we concluded that the noise in magnetometers follow non-Normal distributions as opposed to the common assumption. This conclusion leads to the insight that if Gaussian distribution can fairly model the noise in three axes of magnetometer, the standard deviation of each axis does not need to be equal. In this paper, we propose two methods, the first one assumes different standard deviations on each axis and the second aims to reduce the high computational demand of the first method by converging faster without losing significantly the accuracy.

The main contributions of this paper are introducing the more general assumption of noise in three axes of the magnetometer and proposing a calibration method with significantly lower computational demand that still yields comparable results to the subMLE method.

This paper is organized as follows. Section II formulates the problem under MLE framework. Section III introduces and explains our proposed methods. In Section IV, results from simulations are presented. Finally, Section V summarizes the paper and comments on future work.

II. PROBLEM FORMULATION

A. Problem formulation

Without loss of generality, we assume the magnitude of the geomagnetic field in the navigation frame to be 1. The magnetometer measurements can be modelled by [5]

$$\mathbf{h}_{r,i} = \mathbf{C}\mathbf{R}_i^{nS}\mathbf{h}^n + \mathbf{b} + \mathbf{n}_i, \tag{1}$$

where $\mathbf{h}_{r,i} \in \mathbb{R}^3$ is the reading of magnetometer at time ith, $\mathbf{C} \in \mathbb{R}^{3\times3}$ and $\mathbf{b} \in \mathbb{R}^3$ represent the total transformation and bias respectively, $\mathbf{h}^n$ is the normalized geomagnetic field in the navigation frame, which is assumed to be a constant unit vector, $\mathbf{R}_i^{nS} \in \mathbb{R}^{3\times3}$ represents the navigation frame (n) to sensor frame (S) rotation matrix and $\mathbf{n}_i \in \mathbb{R}^3$ is the wideband noise of the sensor. For simplicity, we denote $\mathbf{h}_i^S = \mathbf{R}_i^{nS}\mathbf{h}^n \in S(3)$ where $S(k) = \{\mathbf{x} \in \mathbb{R}^k : \|\mathbf{x}\|^2 = 1\}$.

We assume that noise on each axis can be modelled by a Gaussian distribution with zero mean and covariance matrix $\boldsymbol{\Sigma}$. Previous state-of-the-art papers assume covariance matrix of noise to be $\sigma^2\mathbf{I}$, which have not taken into account the different standard deviation of axes and the correlation between them. The induced noise in the sensor is

$$\mathbf{n}_i \sim N(\mathbf{0}, \boldsymbol{\Sigma}) \overset{(1)}{\Rightarrow} \mathbf{h}_{r,i} \sim N(\mathbf{C}\mathbf{h}_i^S + \mathbf{b}, \boldsymbol{\Sigma}) \tag{2}$$

The Maximum Likelihood Estimation is used to maximize the conditional probability of n observed values given parameters $(\mathbf{C}, \mathbf{b}) \in \mathbb{R}^{3\times3} \times \mathbb{R}^3 := \Theta$ and $\mathbf{h}_i^S \in S(3), i = 1, ..., n$. The MLE is formulated as

$$\max_{\substack{(\mathbf{C},\mathbf{b})\in\Theta \\ \mathbf{h}_i^S\in S(3), i=1,...,n}} p\{\mathbf{h}_{r,i}|\mathbf{C}, \mathbf{h}_i^S, \mathbf{b}\}$$

$$\overset{\varepsilon_i = \mathbf{h}_{r,i} - \mathbf{C}\mathbf{h}_i^S - \mathbf{b}}{\underset{i.i.d.}{=}} \max_{\substack{(\mathbf{C},\mathbf{b})\in\Theta \\ \mathbf{h}_i^S\in S(3)}} \prod_{i=1}^n \frac{e^{-\frac{1}{2}\varepsilon_i^T(\Sigma)^{-1}\varepsilon_i}}{\left((2\pi)^3 |\boldsymbol{\Sigma}|\right)^{1/2}}$$

$$\overset{\varepsilon_i = \mathbf{h}_{r,i} - \mathbf{C}\mathbf{h}_i^S - \mathbf{b}}{=} \min_{\substack{(\mathbf{C},\mathbf{b})\in\Theta \\ \mathbf{h}_i^S\in S(3)}} \sum_{i=1}^n \varepsilon_i^T(\Sigma)^{-1}\varepsilon_i \tag{3}$$

The solution $(\hat{\mathbf{C}}, \hat{\mathbf{b}}, \widehat{\mathbf{h}_i^S}), i = 1, ..., n$ of (3) is not unique. Assume that the set $(\hat{\mathbf{C}}, \hat{\mathbf{b}}, \widehat{\mathbf{h}_i^S}), i = 1, ..., n$ is a solution, any set of parameters $(\hat{\mathbf{C}}', \hat{\mathbf{b}}, \widehat{\mathbf{h}_i^{S}}'), i = 1, ..., n$ is also a solution if $\hat{\mathbf{C}}' = \hat{\mathbf{C}}\mathbf{R}^T$ and $\widehat{\mathbf{h}_i^{S}}' = \mathbf{R}\widehat{\mathbf{h}_i^S}$ where $\mathbf{R}$ is an orthonormal matrix. Thus, the calibration of magnetometers is usually divided into two steps [5]

1. *Transform measurements from ellipsoid to sphere*: Find parameters $(\mathbf{C}, \mathbf{b}) \in \Theta$ and transform measurements from ellipsoidal manifold to spherical manifold by $\mathbf{h}_i^F = \mathbf{C}^{-1}(\mathbf{h}_{r,i} - \mathbf{b})$ where F denotes some transformation frame.

2. *Align measurements from F frame to sensor frame S*: Find the rotation matrix $\mathbf{R}^{FS}$ by using magnetic field measurements $\mathbf{h}_i^S$ obtained from the external information sources. The procedure is described in detail in [5].

III. PROPOSED METHOD

After dividing the calibration into two steps, our objective function for the first step becomes

$$\min_{\substack{(\mathbf{C},\mathbf{b})\in\Theta, \ \mathbf{h}_i^F\in S(3) \\ \varepsilon_i = \mathbf{h}_{r,i} - \mathbf{C}\mathbf{h}_i^F - \mathbf{b}}} \sum_{i=1}^n \varepsilon_i^T(\Sigma)^{-1}\varepsilon_i \tag{4}$$

Solving the minimization problem (4) indicates that we need to estimate n auxiliary magnetic field vectors $\mathbf{h}_i^F$ and our calibration parameter space is only $\dim(\Theta) = 12$ while the search space is (2n+12). If the unit vectors $\mathbf{h}_i^F$ can be approximated by methods with low computational complexity, the search space and complexity of (4) are reduced. One approach to solve this is to use the parameters $(\mathbf{C}_{LS}, \mathbf{b}_{LS}) \in \Theta$ estimated by Least Square procedure and implemented in [4], then transform the measurement vectors $\mathbf{h}_{r,i}$ to unit sphere. Our proposed algorithm for transforming measurements from ellipsoid to sphere is described in Algorithm 1.

ALGORITHM 1. TRANSFORM MEASUREMENTS FROM ELLIPSOID TO SPHERE WITH ARTIFICIAL DATA CREATION

Input: Magnetometer measurements at index *ith* $\mathbf{h}_{r,i}$.
Output: Calibration parameters $\hat{\mathbf{C}}, \hat{\mathbf{b}}$ and transformed magnetic field measurements $\mathbf{h}_i^F$

1. Estimate $(\mathbf{C}_{LS}, \mathbf{b}_{LS}) \in \Theta$ in [4]
2. Create an artificial geomagnetic field
   $\mathbf{h}_{LS,i}^F = \mathbf{C}_{LS}^{-1}(\mathbf{h}_{r,i} - \mathbf{b}_{LS})$
3. Normalize the created geomagnetic field to fulfill the condition $\mathbf{h}_i^F \in S(3)$ by
   $$\mathbf{h}_{LS,i}^F = \frac{\mathbf{h}_{LS,i}^F}{\|\mathbf{h}_{LS,i}^F\|}$$
4. A. Estimate the covariance matrix $\hat{\boldsymbol{\Sigma}}$ of noise by following procedure in [8].
   Estimate the parameters $\hat{\mathbf{C}}, \hat{\mathbf{b}}$ from solving the optimization problem by iterative method
   $$\text{ADC1:} \min_{\substack{(\mathbf{C},\mathbf{b})\in\Theta \\ \varepsilon_i = \mathbf{h}_{r,i} - \mathbf{C}\mathbf{h}_{LS,i}^F - \mathbf{b}}} \sum_{i=1}^n \varepsilon_i^T(\hat{\Sigma})^{-1}\varepsilon_i$$
   B. Iteratively solve the following problem to estimate the parameters $\hat{\mathbf{C}}, \hat{\mathbf{b}}$
   $$\text{ADC2:} \min_{\substack{(\mathbf{C},\mathbf{b})\in\Theta \\ \varepsilon_i = \mathbf{h}_{r,i} - \mathbf{C}\mathbf{h}_{LS,i}^F - \mathbf{b}}} \sum_{i=1}^n \varepsilon_i^T\varepsilon_i$$
5. Calculate the transformed magnetic field measurements
   $$\mathbf{h}_i^F = \hat{\mathbf{C}}^{-1}(\mathbf{h}_{r,i} - \hat{\mathbf{b}})$$

In Algorithm 1, Artificial Data Creation 1 (ADC1) uses the objective function that was discussed previously while Artificial Data Creation 2 (ADC2) ignores the covariance matrix of noise in sensor. In this paper, both methods are implemented to compare their performance in estimating parameters. An initial guess to solve the iterative optimization problem is produced by the Least Square method in [4]. Applying Singular Value Decomposition to the estimated parameter $\hat{\mathbf{C}} = \mathbf{U}\mathbf{S}\mathbf{V}^T$, we can use $\mathbf{S}$ and $\mathbf{R} = \mathbf{U}$

to evaluate the performance of calibration algorithms in estimating **S** (Scaling) and **R** (Rotation) separately [5]. Next, simulation results are presented to demonstrate the effect of our proposed calibration procedure.

IV. SIMULATION RESULTS

A. Estimation of calibration parameters

A simulated set of 1000 data points is used to analyze the performance of the calibration algorithm. Chosen calibration parameters are

$$\mathbf{C} = \begin{bmatrix} 31.90 & -40.15 & 19.80 \\ 46.75 & 9.37 & -1.19 \\ -17.19 & 44.30 & 35.60 \end{bmatrix}, \mathbf{b} = \begin{bmatrix} 13.5 \\ 4.14 \\ 7.54 \end{bmatrix} \mu T$$

$$\Sigma = \begin{bmatrix} 25 & -1 & 0.16 \\ -1 & 49 & -1.44 \\ 0.16 & -1.44 & 100 \end{bmatrix} \times 10^{-2} \ \mu^2 T^2, \mathbf{h}^n = \begin{bmatrix} 0 \\ 0 \\ 55 \end{bmatrix} \mu T$$

The attitude matrix $\mathbf{R}_i^{nS}$ is parameterized in Euler angles with the three angles given as functions of index i (for simplicity, i is omitted in the following equation)

$$\mathbf{R}_i^{nS} = \begin{bmatrix} \cos\psi \cos\theta & -\sin\psi & \cos\psi \sin\phi \\ \sin\phi \sin\theta + \cos\phi \cos\theta \sin\psi & \cos\phi \cos\psi & \cos\phi \sin\theta \sin\psi - \sin\phi \cos\theta \\ \sin\phi \cos\theta \sin\psi - \sin\theta \cos\phi & \sin\phi \cos\psi & \cos\phi \cos\theta + \sin\phi \sin\theta \sin\psi \end{bmatrix}$$

where

$$\begin{cases} \phi_i (\text{roll}) = 0 \\ \theta_i(\text{pitch}) = \left(\frac{i}{100} - \left\lfloor \frac{i}{100} \right\rfloor \right) \pi \quad (\text{unit: rad}) \\ \psi_i(\text{yaw}) = 0.2\pi \lfloor i/100 \rfloor \end{cases},$$

and $\lfloor x \rfloor$ is the function that outputs the greatest integer less than or equal to x.

To facilitate the performance comparison between different methods, the error metrics described in [5] is applied

$$e_b = \| \mathbf{b} - \hat{\mathbf{b}} \|_2, e_S = \| \mathbf{S} - \hat{\mathbf{S}} \|_{Fro}, e_R = \cos^{-1}\left(\frac{tr(\mathbf{R}\hat{\mathbf{R}}) - 1}{2} \right),$$

where $\mathbf{X}, \hat{\mathbf{X}}$ denotes the true and estimated parameters.

We ran 100 Monte Carlo simulations for the above calibration and noise parameters in Matlab [9]. The Quasi-Newton algorithm is implemented in a laptop with an i5-7200U 2.5 GHz processor. The stop condition of the minimization problem is Step Size < 10-6. Table I shows the mean and standard deviations of error metrics defined above for Least Square (LS) method [4], the reference subMLE [5] and our two proposed methods. The time required for executing step 1 to 4 in Algorithm 1 is presented in the table.

ADC1 method yields the most accurate parameter estimates for **b** and **R** while ADC2 yields the best estimate for **S**. However, the differences between estimates from subMLE, ADC1 and ADC2 are rather small. All three methods yield approximately 11% more accurate estimates for **S** and approximately 3% better estimates for **R** than the LS approach. These results show that all three methods transform the ellipsoid to sphere better than LS method. Although ADC1 yields more accurate estimates for two of the three parameters, ADC2 is the better choice as it provides estimates that are similarly good and is significantly faster than ADC1 and subMLE. ADC2 is almost 20 times faster

TABLE I. CALIBRATION ERROR METRICS AND TIME. MEAN ERRORS AND STANDARD DEVIATION IN (.) FOR PARAMETERS **B**, **S** AND **R**. LAST COLUMN SHOWS RUN TIME OF EACH METHOD IN SECONDS AND RELATIVE COMPARISION TO LS IN [.]. **BOLD** INDICATE THE SMALLEST MEAN ERROR FOR A PARTICULAR PARAMETER ESTIMATE.

	e_b	e_S	e_R	Time (s)
LS	0.0866 (0.0387)	0.1364 (0.0510)	0.0042 (0.0018)	0.0020
subMLE	0.0866 (0.0387) [−2e(−7)]	0.1214 (0.0541) [−0.1096]	0.0041 (0.0018) [−0.0299]	1.4221 [711.05]
ADC1	**0.0866** (0.0387) [−2e(−7)]	0.1217 (0.0584) [−0.1078]	**0.0040** (0.0018) [−0.0336]	0.6502 [325.10]
ADC2	0.0866 (0.0387) [−1e(−7)]	**0.1208** (0.0577) [−0.1142]	0.0041 (0.0018) [−0.0312]	**0.0328** [16.40]

than ADC1 and 43 times faster than subMLE. Since this paper paper focuses on sensors used in smartphones, which have limited computational resources, ADC2 is used in the next subsection to evaluate the accuracy in estimating the heading angle of the device.

B. Estimation of Heading angle

Magnetometer can be used for heading estimation. Simulation procedure is created with 101 Monte Carlo runs for the following settings defined in Matlab [9]:

measurement range: 200, resolution: 0.0625,

constant bias: [2 -3 1], axes misalignment: [20 40 3],

noise density: [0.15 0.15 0.2], sampling period of 15ms.

The magnetometer is rotated by three axes in the navigation frame, three times for each axis as shown in Fig. 1. In those 101 runs, the alignment matrix from F frame to S frame [5] is estimated by the first run with the given magnetic field in frame S and used for all 100 left runs. This simulation procedure imitates a real scenario in which the true heading information is not provided all the time. The heading angle ϕ in S frame is calculated by

$$\phi = \tan^{-1}(h_y/h_x),, \quad (5)$$

where h_x and h_y are magnetic field measurements in x and y direction of frame S. If $\phi = 0$, the x-axis points to the magnetic North, the z-axis points downward and y-axis completes the right-hand rule.
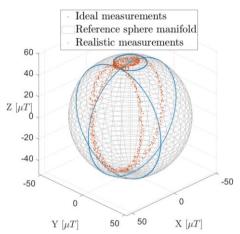

Fig. 1. Measurements from the ideal magnetometer (no error) and realistic magnetometer (with the above settings)

The data from rotating the sensor horizontally (around the z-axis) is used to estimate the heading angle by (5). The absolute error in heading angle estimation by raw measurements and calibrated ones from LS, subMLE and ADC2 are shown in Table II. ADC2 yields more accurate heading angle estimates than both LS and subMLE. Furthermore, it is again significantly faster than subMLE. Smoothing can be applied to denoise the measurements after they have been calibrated by ADC2. The smoothing windows of length 3 to 67 were evaluated, and with window length 15 the lowest heading error was achieved.

The calibrated magnetometer data yielded by ADC2 are compared to the raw data in Fig. 2. The calibrated readings are near to the unit circle locus, which validates that the combined effect of the magnetic distortions is successfully compensated.

V. CONCLUSION

It is also shown that the proposed methods reduce considerably the search space for the parameters that have to be estimated for magnetometer calibration problem. ADC1 and ADC2 yield parameter estimates that are approximately accurate as the estimates of the state-of-the-art method subMLE while outperforming the LS method in terms of accuracy. Most importantly, both methods are significantly faster than the subMLE method, and ADC2 is significantly faster than ADC1. ADC2 is not only faster than ADC1 in computational time but it is also faster to implement since it does not require estimation of the covariance matrix, however, one needs to choose the method depending on the computational time or the accuracy of parameter they want to estimate. In this paper, the authors choose ADC2 since the aim was to calibrate magnetometers integrated in devices with low computational resources. The heading angle estimation using the ADC2 method also showed an approximately 0.5% improvement compared to LS or subMLE. This small improvement has greater impact when using IMUs for real time Pedestrian Dead Reckoning applications, where small errors in the heading estimate can quickly cause large positioning errors.

The intuition behind the proposed methods is from comparing the standard deviation of noise in axes of magnetometer with the magnitude of geomagnetic field at the experimental location. It is observed, e.g. in [10] that the magnitude of geomagnetic field is around 55 µT while the standard deviation of noise in one axis is approximately 0.35 µT (less than 100 times). Thus, the transformed magnetic field from ellipsoid to unit sphere is sufficiently close to $\mathbf{h}_i^S$ after a rotation.

TABLE II. MEAN OF 100 MONTE CARLO RUNS IN ESTIMATING HEADING ANGLE ERRORS AND COMPUTATIONAL TIME

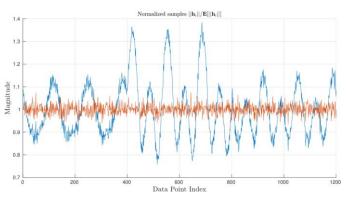|	Heading error (0)	Calibration time (s)
Raw	29.3803	
LS	8.8760	0.0039
subMLE	8.8789	2.1799
ADC2	8.8284	0.0603
ADC2 smooth	7.3883	

Fig. 2. Norm of calibrated data (orange) compared to raw data (blue)

In the future the proposed methods will be tested and compared with LS and subMLE using real-world data from both magnetometers integrated in smartphones and more reliable magnetometers integrated in, e.g., XSens units.

REFERENCES

[1] P. Müller, M. Raitoharju, S. Ali-Löytty, L. Wirola, R. Piche. "A survey of parametric fingerprint-positioning methods," Gyroscopy and Navigation, vol. 7(2), 2016, pp. 107-127.

[2] J. Collin, P. Davidson, M. Kirkko-Jaakkola, H. Leppäkoski, "Inertial sensors and their applications," Handbook of Signal Processing Systems, 3 ed. Springer, 2019. p. 51-85

[3] D. Gebre-Egziabher, G. H. Elkaim, J. D. Powell, and B.W. Parkinson, "Calibration of strapdown magnetometers in magnetic field domain," Journal of Aerospace Engineering, vol. 19(2), April 2006, pp.87-102.

[4] A. Barraud. "Least square magnetic calibration toolbox," available at: https://se.mathworks.com/matlabcentral/fileexchange/23398-magnetometers-calibration?stid=profcontriblnk

[5] J. F. Vasconcelos, G. Elkaim, C. Silvestre, P. Oliveira and B. Cardeira, "Geometric approach to strapdown magnetometer calibration in sensor frame," IEEE Transactions on Aerospace and Electronic Systems, vol. 47, no. 2, April 2011, pp. 1293-1306.

[6] Y. Wu and W. Shi, "On calibration of three-axis magnetometer," IEEE Sensors Journal, vol. 15(11), 2015, pp.6424-6431

[7] M. Kok, T.B. Schön, "Magnetometer calibration using inertial sensors," IEEE Sensors Journal. 2016 May 16;16(14):5679-89

[8] N. Nguyen, P. Müller and J. Collin, "The statistical analysis of noise in triaxial magnetometers and calibration procedure" 2019 16th Workshop on Positioning, Navigation and Communications (WPNC), Bremen, 2018, pp. 1-6, in press

[9] MATLAB, ver. 9.6.0.1072779 (R2019a), pub. The MathWorks Inc.

[10] Nhan Nguyen, "The statistical analysis of noise in triaxial sensor", Bachelor's Thesis, Tampere, Tampere University, 2019. Available: http://urn.fi/URN:NBN:fi:tuni-20190905316